Phytochemistry 186 (2021) 112738

Contents lists available at ScienceDirect

Phytochemistry

journal homepage: www.elsevier.com/locate/phytochem

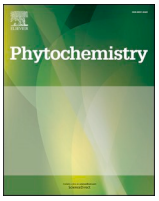

3-*O*-glycosylation of kaempferol restricts the supply of the benzenoid precursor of ubiquinone (Coenzyme Q) in *Arabidopsis thaliana*

Eric Soubeyrand [a], Scott Latimer [a], Ann C. Bernert [a], Shea A. Keene [b], Timothy S. Johnson [b], Doosan Shin [a], Anna K. Block [c], Thomas A. Colquhoun [b], Anton R. Schäffner [d], Jeongim Kim [a,**], Gilles J. Basset [a,*]

[a] Department of Horticultural Sciences, University of Florida, Gainesville, FL, 32611, USA
[b] Department of Environmental Horticulture, Plant Innovation Center, Institute of Food and Agricultural Sciences, University of Florida, Gainesville, FL, 32611, USA
[c] Center for Medical, Agricultural and Veterinary Entomology, U.S. Department of Agriculture-Agricultural Research Service, Gainesville, FL, 32608, USA
[d] Institute of Biochemical Plant Pathology, Helmholtz Zentrum München, German Research Center for Environmental Health, D-85764, Neuherberg, Germany

ARTICLE INFO

Keywords: *Arabidopsis thaliana* Brassicaceae
Metabolism
Functional genomics
Benzoquinones
Flavonoids
Benzoates
Ubiquinone
Kaempferol
4-hydroxybenzoate
UDP-carbohydrate-dependent glycosyltransferases

ABSTRACT

Ubiquinone (Coenzyme Q) is a vital respiratory cofactor and antioxidant in eukaryotes. The recent discovery that kaempferol serves as a precursor for ubiquinone's benzenoid moiety both challenges the conventional view of flavonoids as specialized metabolites, and offers new prospects for engineering ubiquinone in plants. Here, we present evidence that *Arabidopsis thaliana* mutants lacking kaempferol 3-*O*-rhamnosyltransferase (*ugt78d1*) and kaempferol 3-*O*-glucosyltransferase (*ugt78d2*) activities display increased *de novo* biosynthesis of ubiquinone and increased ubiquinone content. These data are congruent with the proposed model that unprotected C-3 hydroxyl of kaempferol triggers the oxidative release of its B-ring as 4-hydroxybenzoate, which in turn is incorporated into ubiquinone. Ubiquinone content in the *ugt78d1/ugt78d2* double knockout represented 160% of wild-type level, matching that achieved via exogenous feeding of 4-hydroxybenzoate to wild-type plants. This suggests that 4-hydroxybenzoate is no longer limiting ubiquinone biosynthesis in the *ugt78d1/ugt78d2* plants. Evidence is also shown that the glucosylation of 4-hydroxybenzoate as well as the conversion of the immediate precursor of kaempferol, dihydrokaempferol, into dihydroquercetin do not compete with ubiquinone biosynthesis in *A. thaliana*.

1. Introduction

Ubiquinone (Coenzyme Q) is a lipophilic redox cofactor that functions as an essential electron carrier in the respiratory chain of eukaryotes and many prokaryotes (Brandt and Trumpower, 1994; Bentinger et al., 2010; Nowicka and Kruk, 2010). Furthermore, together with tocopherols, carotenoids and estrogens, ubiquinone is one of the major liposoluble antioxidants in eukaryotes (Bentinger et al., 2007, 2010), and there is consequently interest in exploiting its free-radical scavenging properties to engineer resistance to abiotic stresses in plants (Ohara et al., 2004; Liu et al., 2019).

Ubiquinone is a bipartite molecule, made up of benzoquinone and prenyl moieties (Fig. 1). In flowering plants, it is now established that the direct precursor for the benzoquinone backbone is 4-hydroxybenzoate and that the latter originates predominantly from the metabolism of *p*-coumarate (Block et al., 2014; Soubeyrand et al., 2019). The conversion of *p*-coumarate into 4-hydroxybenzoate occurs via at least two pathways (Fig. 1). The first pathway takes place in peroxisomes and entails β-oxidation of the propyl side-chain of *p*-coumarate (Block et al., 2014; Soubeyrand et al., 2019). In the second pathway, cytosolic *p*-coumarate is first incorporated into kaempferol (B-ring), the catabolism of which then releases 4-hydroxybenzoate (Soubeyrand et al., 2018). Mitochondria, where ubiquinone assembly takes place, can import 4-hydroxybenzoate from either pathway (Fig. 1).

In *Arabidopsis thaliana* (L.) Heynh (Brassicaceae) the β-oxidation of *p*-coumarate is the major supplier of 4-hydroxybenzoate for ubiquinone

Abbreviations: HPLC, High performance liquid chromatography; Liquid chromatography-tandem mass spectrometry, LC-MS/MS; UDP, Uridine diphosphate; UDP-carbohydrate-dependent glycosyltransferase, UGT.

* Corresponding author.
** Corresponding author.
E-mail address: gbasset@ufl.edu (G.J. Basset).

https://doi.org/10.1016/j.phytochem.2021.112738
Received 15 December 2020; Received in revised form 8 March 2021; Accepted 9 March 2021
Available online 21 March 2021

biosynthesis (Soubeyrand et al., 2018). Yet, because the pool of kaempferol far exceeds that of ubiquinone — *e.g.* ~400 nmol g^{-1} of fresh weight vs. 2–3 nmol g^{-1} of fresh weight in *A. thaliana* leaves (Yin et al., 2012; Block et al., 2014; Soubeyrand et al., 2018) — one can presume that even a modest increase in kaempferol turnover would dramatically boost ubiquinone levels. The catabolism of kaempferol could therefore represent an opportunity for ubiquinone engineering in plant tissues.

In vitro enzymatic assays using *A. thaliana* leaf extracts suggest that the release of 4-hydroxybenzoate from kaempferol is catalyzed by one or more heme-dependent peroxidases (Fig. 1; Soubeyrand et al., 2018). Importantly, the chemistry of this reaction requires a free hydroxyl group on C-3 of the C-ring of kaempferol (Fig. 1; Soubeyrand et al., 2018). This feature is of particular physiological significance because in most plant tissues kaempferol is glycosylated on its C-3 hydroxyl position (Fig. 1; Lepiniec et al., 2006; Yonekura-Sakakibara et al., 2008; Buer et al., 2013) and is therefore refractory to peroxidative cleavage. Indirectly confirming this premise, *in vitro* assays indicated that peroxidase activities are so high in *A. thaliana* that they could wipe out the entire pool of kaempferol of leaf tissues in minutes should its C-3 hydroxyl not be protected (Soubeyrand et al., 2018). In the context of ubiquinone biosynthesis and its engineering, this suggests that a large pool of benzenoid precursor is immobilized in the form of kaempferol-3-*O*-glycosides and that the corresponding glycosyltransferases act as a control point on the pathway.

The aim of this study was therefore two-fold: first, determine to what extent the supply of 4-hydroxybenzoate restricts ubiquinone biosynthesis in plant tissues. Second, test by means of reverse genetics if 4-hydroxybenzoate can be reclaimed from the pools of kaempferol-3-*O*-glycosides to boost ubiquinone content.

2. Results and discussion

2.1. The exogenous supply of 4-hydroxybenzoate boosts ubiquinone-9 content in *A. thaliana*

To determine if the supply of the ring precursor limits ubiquinone biosynthesis in plants, and if so to what extent, ubiquinone-9 content was quantified in *A. thaliana* plants axenically fed for 24h with various concentrations of 4-hydroxybenzoate (Fig. 2). Feeding assays at 2 and 10 μM of 4-hydroxybenzoate resulted in a 120–135% increase in ubiquinone-9 content in rosette leaves as compared to control plants with no 4-hydroxybenzoate supplementation (Fig. 2). At 125 and 250 μM of 4-hydroxybenzoate, ubiquinone-9 content in rosette leaves further increased to plateau at approximately 150% of ubiquinone-9 level in the controls (Fig. 2). These data indicate that in *A. thaliana* leaf tissues, as in yeast and mammals (Pierrel et al., 2010; Fernández-del-Río et al., 2017, 2020), the availability of 4-hydroxybenzoate can limit ubiquinone biosynthesis. Notably, experiments conducted with

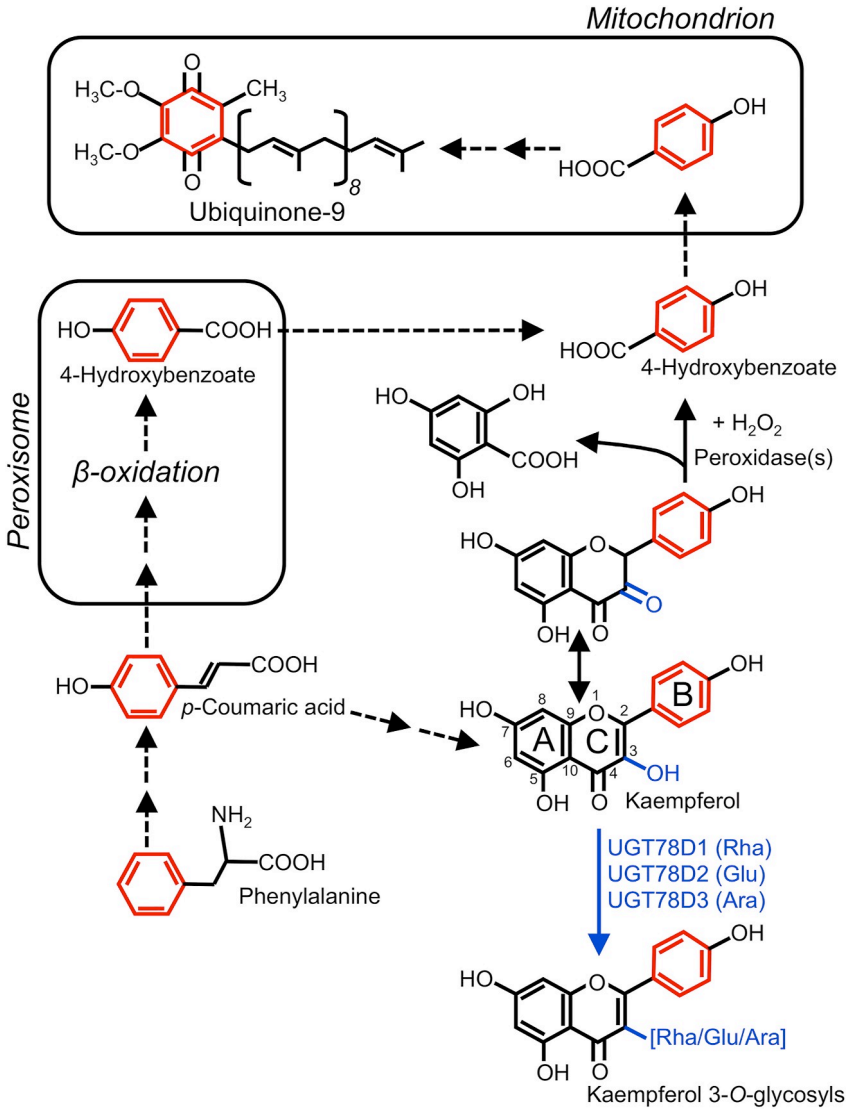

Fig. 1. Metabolic origins of 4-hydroxybenzoate for ubiquinone biosynthesis in plant cells. Note that chemical modeling of the peroxidative cleavage of kaempferol predicts that peroxidases do not act on kaempferol itself, but on its α-diketone tautomer. The formation of the latter is contingent on the presence of a double bond between C-2 and C-3 and a free C-3-OH on the C-ring. Dashed arrows indicate unknown and/or multiple steps. Ara, arabinosyl; Glu, glucosyl; Rha, Rhamnosyl; UGT78D1, flavonol 3-*O*-rhamnosyltransferase; UGT78D2, flavonol 3-*O*-glucosyltransferase; UGT78D3, flavonol 3-*O*-arabinosyltransferase.

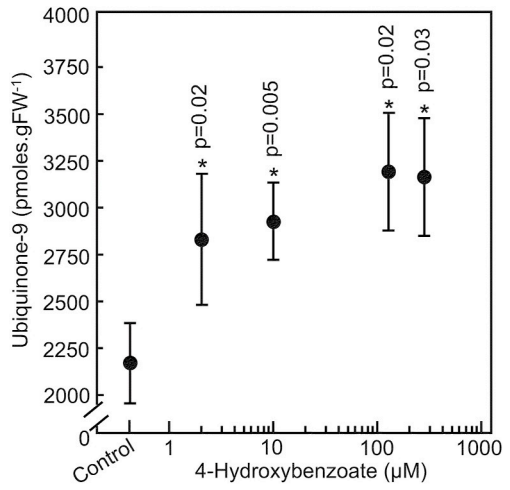

Fig. 2. Ubiquinone-9 levels in *A. thaliana* rosette leaves. *A. thaliana* seedlings were axenically fed for 24h with 0 (control), 2, 10, 125 and 250 µM of 4-hydroxybenzoate. Data represent the means of 5 biological replicates ± SE. P values from an analysis of variance between each mutant and the wild-type reference are indicated above the bars. Asterisks indicate significant differences between the control and the 4-hydroxybenzoate-fed plants as determined by variance analysis ($P < \alpha = 0.1$).

mammalian cell cultures indicated that this bottleneck on ubiquinone biosynthesis was cell type dependent (Fernández-del-Río et al., 2017). For instance, kidney cells cultured in presence of 4-hydroxybenzoate accumulated up to six times more ubiquinone than the controls, while liver-derived cells displayed little or no increase in ubiquinone content in response to 4-hydroxybenzoate supplementation (Fernández-del-Río et al., 2017). Consequently, a conservative interpretation of our results is that the 4-hydroxybenzoate-induced boosts in ubiquinone-9 level correspond to average values of the multiple cellular types that make up the leaf tissues.

An additional and crucial finding from these feeding assays is that *A. thaliana* is an appropriate system to genetically test the proposed model for the oxidative catabolism of kaempferol in plants: an increase in the *in vivo* level of 4-hydroxybenzoate resulting from increased kaempferol cleavage being indeed likely to translate into a boost in ubiquinone content in leaf tissue.

2.2. Loss of kaempferol 3-O-glycosyltransferase activities stimulates ubiquinone biosynthesis in A. thaliana leaf tissues

The current model for the incorporation of the B-ring of kaempferol into ubiquinone postulates that the *in vivo* glycosylation of kaempferol on its C-3 hydroxyl prevents the oxidative release of the B-ring as 4-hydroxybenzoate and thus its incorporation into ubiquinone (Soubeyrand et al., 2018). To test this scenario, the ubiquinone-9 content and rate of *de novo* biosynthesis of *A. thaliana* leaf tissues were investigated in knockout mutants corresponding to the three UDP-carbohydrate-dependent glycosyltransferases (UGTs) known to act on the C-3 hydroxyl of kaempferol (Fig. 1): UGT78D1 (flavonol 3-*O*-rhamnosyltransferase; At1g30530), UGT78D2 (flavonol 3-*O*-glucosyltransferase; At5g17050), and UGT78D3 (flavonol 3-*O*-arabinosyltransferase; At5g17030) (Jones et al., 2003; Tohge et al., 2005; Yonekura-Sakakibara et al., 2007, 2008; Yin et al., 2012). Because in leaf tissues UGT78D1 and UGT78D2 bear most of the kaempferol 3-O-glycosyltransferase activities (Jones et al., 2003; Tohge et al., 2005; Yonekura-Sakakibara et al., 2008) and compete with each other for kaempferol usage (Yin et al., 2012), an *ugt78d1/ugt78d2* double knockout was also included in our analyses. HPLC analysis showed that the total ubiquinone-9 content in the leaf extracts of the *ugt78d2* and *ugt78d1/ugt78d2* knockout plants was 123% and 160% of that of their wild-type counterpart, respectively (Fig. 3A). No statistically significant differences were observed between the total ubiquinone-9 content of the *ugt78d1* and *ugt78d3* knockouts as compared to the wild-type plants (Fig. 3A).

Measurement of the rates of *de novo* ubiquinone biosynthesis using LC-MS/MS quantification of the incorporation of pulse-fed phenylalanine-[*Ring*$^{13}C_6$] into ubiquinone-9 recapitulated in part these results. The rate of isotopic enrichment of ubiquinone-9 in the *ugt78d1/ugt78d2*

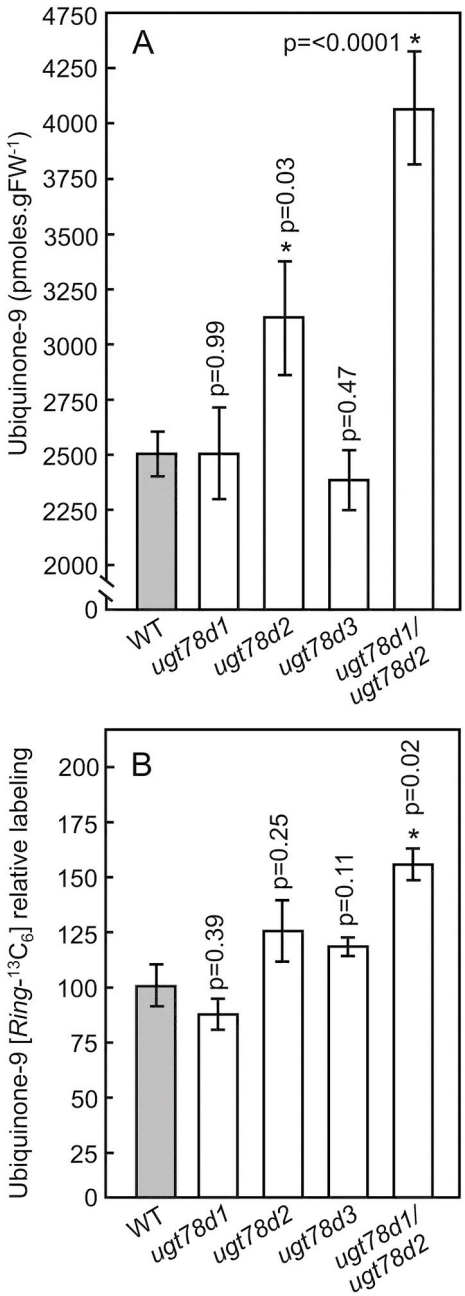

Fig. 3. Total ubiquinone content and rate of *de novo* ubiquinone biosynthesis in *A. thaliana*. A) Total ubiquinone-9 content in the rosette leaves of 3-week-old wild-type, *ugt78d1*, *ugt78d2*, *ugt78d3* and *ugt78d1/ugt78d2* plants grown on soil. B) Relative ubiquinone-9- [*Ring*-$^{13}C_6$] labeling in the leaves of axenically grown wild-type, *ugt78d1*, *ugt78d2*, *ugt78d3 and ugt78d1/ugt78d2* plants fed for 3h with 250 µM of phenylalanine-[*Ring*-$^{13}C_6$]. Data represent the means of 4–6 biological replicates ± SE. P values from an analysis of variance between each mutant and the wild-type reference are indicated above the bars. Asterisks indicate significant differences from the wild type as determined by variance analysis ($P < \alpha = 0.1$).

double knockout was 157% of that of wild-type plants (Fig. 3B). Measured rates of *de novo* ubiquinone biosynthesis were also higher in the *ugt78d2* and *ugt78d3* knockouts as compared to wild-type plants (26% and 20% higher, respectively), but the statistical confidence for these differences was below the significance threshold (Fig. 3B). No statistically significant difference in the *de novo* biosynthesis of ubiquinone-9 was observed either between the *ugt78d1* knockout and the wild type (Fig. 3B).

These results validate the model that, in the *ugt78d1/ugt78d2* plants, where the majority of kaempferol 3-*O*-glycosyltransferase activities are lacking, de-protection of the C-3 hydroxyl of kaempferol triggers the release of the B-ring of kaempferol as 4-hydroxybenzoate and thus boosts ubiquinone-9 biosynthesis. These data are also consistent with our previous report that kaempferol-3-*O*-glucoside is resistant to cleavage by heme-dependent peroxidases *in vitro* (Soubeyrand et al., 2018).

2.3. The ugt78d1/ugt78d2 knockout does not display increased levels of 4-hydroxybenzoate conjugates

Plant tissues are well known to actively glucosylate 4-hydroxybenzoate either on its 4-hydroxyl group or on its carboxyl group, leading to the formation of 4-*O*-(1-β-D-glucosyl) benzoate and 4-hydroxybenzoate 1-β-D-glucose ester, respectively (Cooper-Driver et al., 1972; Klick and Herrmann, 1988; Siebert et al., 1996). In *A. thaliana*, *in vitro* assays of recombinant UGTs with 4-hydroxybenozoate as a substrate have shown that at least 5 UGTs can form 4-*O*-(1-β-D-glucosyl) benzoate — interestingly, UGT78D2 is one of those — and at least 3 others can form the glucose ester variant (Lim et al., 2002). These *O*-glucoside derivatives are most likely sequestered in the vacuole (Yazaki et al., 1995), where one can assume they do not participate in the biosynthesis of ubiquinone.

HPLC analyses indicated that methanol extracts of roots and leaves of wild-type and *ugt78d1/ugt78d2* plants did not contain any detectable amount of free 4-hydroxybenzoate (Fig. 4). In contrast, after acidic hydrolysis of the same extracts, 4-hydroxybenzoate was readily detected, demonstrating that most, if not all, of 4-hydroxybenzoate in *A. thaliana* occurs as conjugated derivatives (Fig. 4). These data agree with the previous observation that much of 4-hydroxybenzoate in tobacco leaves is glucosylated (Siebert et al., 1996). Importantly, the amounts of 4-hydroxybenzoate measured in the acid-treated extracts from the *ugt78d1/ugt78d2* knockout were not statistically different from those of wild-type plants (Fig. 4). These results show that in the *ugt78d1/ugt78d2* mutant the higher susceptibility of kaempferol to oxidative cleavage does not result in an increased sequestration of 4-hydroxybenzoate. On a side note, our data also indicate that loss of function of *UGT78D2* has no significant effect on the glucosylation level of 4-hydroxybenzoate *in vivo*, even if the cognate enzyme can form 4-*O*-(1-β-D-glucosyl) benzoate *in vitro* (Lim et al., 2002).

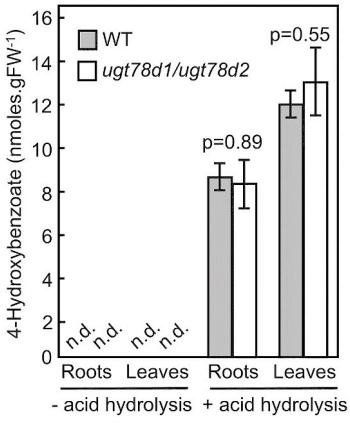

Fig. 4. 4-hydroxybenzoate content in *A. thaliana* roots and rosette leaves. Roots were harvested from 17-day-old axenic cultures, while rosette leaves were harvested from 3-week-old plants grown on soil. Samples were processed with and without acidic hydrolysis, and 4-hydroxybenzoate was quantified by HPLC-spectrophotometry. Data represent the means of 3–4 biological replicates ± SE. P values from an analysis of variance between the *ugt78d1/ugt78d2* knockout and the wild-type reference are indicated above the bars. Threshold for statistically significant differences between *ugt78d1/ugt78d2* and wild-type data as determined by variance analysis was $P < \alpha = 0.1$. n.d.: not detected.

2.4. Loss of function of flavonoid 3′-hydroxylase has no impact on ubiquinone content

Flavonoid 3′-hydroxylase (At5g07990) catalyzes the conversion of dihydrokaempferol, the direct precursor of kaempferol, into dihydroquercetin (Schoenbohm et al., 2000; Supplementary Fig. 1). To determine if the activity of this enzyme competes with the production of deglucosylated kaempferol for ubiquinone biosynthesis, the ubiquinone-9 content in the rosette leaves of the *ugt78d2* knockout was compared to that of an *ugt78d2/f3′h* double knockout. The *f3′h* single knockout and the wild type served as references. No statistically significant differences in ubiquinone-9 content was observed between *f3′h* and wild-type plants (Fig. 5), confirming our previous observation that blockage of the flavonoid biosynthetic pathway downstream of dihydrokaempferol and dihydroquercetin had no effect on ubiquinone accumulation in *A. thaliana* (Soubeyrand et al., 2018). As expected, the ubiquinone-9 content in the leaves of the *ugt78d2/f3′h* and *ugt78d2* knockouts was higher than that in wild-type plants, but no statistically significant differences was observed between the *ugt78d2* and *ugt78d2/f3′h* knockouts (Fig. 5). It thus appears that the metabolic branch point created by flavonoid 3′-hydroxylase immediately upstream of kaempferol does not compete with ubiquinone production.

3. Conclusions

Our data provide evidence that blockage of kaempferol 3-*O*-glycosyltransferase activities boosts ubiquinone biosynthesis in *A. thaliana*, and thus genetically validate the proposed mechanism for the release of 4-hydroxybenzoate via the oxidative cleavage of kaempferol. The involvement of peroxidases in this process, though likely and observed *in vitro* (Soubeyrand et al., 2018), remains to be demonstrated *in vivo*. Along this line, one should also mention that owing to its marked hydrophobicity, kaempferol is likely to have very low solubility *in vivo*.

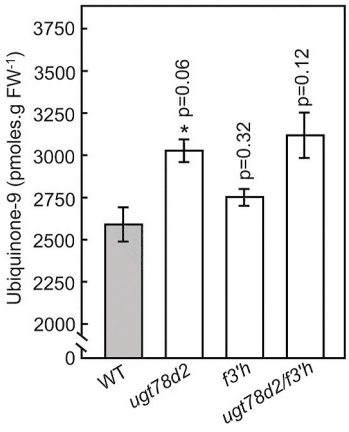

Fig. 5. Total ubiquinone-9 content in the rosette leaves of wild-type, *ugt78d2*, *f3′h, and f3′h/ugt78d2* plants. Plants were grown on soil in 16-h days (110 μE m^{-2} s^{-1}) at 22 °C for 3 weeks. Data represent the means of 7–8 biological replicates ± SE. P values from an analysis of variance between each mutant and the wild-type reference are indicated above the bars. The asterisk indicates significant differences from the wild type as determined by variance analysis ($P < \alpha = 0.1$).

7-*O*-glycosylated versions of kaempferol, which display increased solubility in aqueous solvents, could therefore be the preferred substrates for the peroxidases. *In vitro* assays support this hypothesis (Soubeyrand et al., 2018).

It is noteworthy that the gain in ubiquinone content in the *ugt78d1/ugt78d2* double knockout is two orders of magnitude smaller than that expected if the entire pool of kaempferol present in wild-type *A. thaliana* had been re-routed towards ubiquinone biosynthesis. One may think that because flavonol biosynthesis is repressed in the *ugt78d1/ugt78d2* plants (Yin et al., 2012), the biosynthetic flux of kaempferol itself could in these conditions limit ubiquinone production. This scenario, however, appears to be unlikely because the pool size of kaempferol in the leaves of the *ugt78d1/ugt78d2* plants still dwarfs that of ubiquinone-9 (~80 nmol g^{-1} of fresh weight for kaempferol (Yin et al., 2012) vs. ~4 nmol g^{-1} of fresh weight for ubiquinone-9 (Fig. 3A)). Furthermore, the increase in ubiquinone content in the *ugt78d1/ugt78d2* plants (160% of wild-type level; Fig. 3A) is virtually identical to the maximum boost in ubiquinone-9 level achieved via the exogenous feeding of 4-hydroxybenzoate (150% of the unfed control plants; Fig. 2). Taken together, these observations strongly suggest that the supply of 4-hydroxybenzoate no longer limits ubiquinone-9 biosynthesis in the *ugt78d1/ugt78d2* knockout, and therefore that part of the metabolic control on ubiquinone biosynthesis has shifted to other steps in this pathway. An obvious next phase of engineering to further boost ubiquinone level would be the stacking of this increased supply of 4-hydroxybenzoate with an increased production of ubiquinone side-chain's polyprenyldiphosphate precursor.

4. Experimental

4.1. Chemicals and reagents

Ubiquinone-9 and ubiquinone-10 standards (Sigma-Aldrich) were quantified spectrophotometrically in 100% ethanol using the extinction coefficients of 14,700 M^{-1} cm^{-1} and 14,600 M^{-1} cm^{-1} at 275 nm, respectively (Dawson et al., 1986). Quinol forms (reduced) were prepared by reaction of their corresponding quinone versions with 33 mM of sodium borohydride dissolved in 100% ethanol. 4-Hydroxybenzoate standards (Acros Organics) were prepared in 0.1N HCl and quantified spectrophotometrically using the extinction coefficient of 13,900 M^{-1} cm^{-1} at 255 nm (Dawson et al., 1986). L-Phenylalanine-[*ring*-$^{13}C_6$] was from Cambridge Isotope Laboratories Inc. Murashige and Skoog medium was from MP Biomedicals, LLC. Unless otherwise mentioned, all other chemicals were from Fisher Scientific.

4.2. Plant material and growth conditions

Arabidopsis thaliana (L.) Heynh (Brassicaceae) T-DNA insertion lines *ugt78d1* (SAIL_568F08), *ugt78d2* (SALK_049338), and the double knockout *ugt78d1/ugt78d2* were those described by Yin et al. (2012). The *ugt78d3* knockout line (SALK_114099) was that of Yonekura-Sakakibara et al. (2008). *A. thaliana* T-DNA insertion lines *f3′h* (*tt7*; GK_349F05) and *f3′h/ugt78d2* were those described by Yin et al. (2014). Unless otherwise mentioned, soil-grown plants were subjected to 12-h days (110 µE m^{-2} s^{-1}) at 22 °C using a standard fertilization regime. For the quantification of 4-hydroxybenzoate in rosette leaves, *ugt78d1/ugt78d2* knockout and wild-type plants received an additional high-light treatment for 72h (24h-days; 500 µE m^{-2} s^{-1}) prior to harvesting. For 4-hydroxybenzoate feeding assays, ^{13}C tracer experiments and root harvesting, *A. thaliana* seeds were germinated on Murashige and Skoog agar plates supplemented with 1% (w/v) sucrose. Seven-day-old seedlings were transferred to 250-ml flasks containing 20 ml of Murashige and Skoog medium supplemented with 1% (w/v) sucrose and cultured for an additional 10 days on an orbital shaker (60 rpm) at 22 °C in 10-h days (160 µE m^{-2} s^{-1}). Feeding assays were conducted for 3h (250 µM of phenylalanine-[*Ring*$^{13}C_6$]) or 24h (2, 10, 125 and 250 µM of 4-hydroxybenzoate).

4.3. Ubiquinone extraction and analyses

For the HPLC-diode array quantification of total ubiquinone-9 in *A. thaliana* leaves, 50–120 mg of fresh weight material were spiked with 4.5–5.5 nmoles of ubiquinone-10 as an internal standard, and ground in 0.4 ml of 95% (vol/vol) ethanol using a 5-ml Pyrex tissue grinder. The grinder was then washed twice with 0.3 ml of 95% (vol/vol) ethanol, and the washes were combined with the extract in a 10-ml pyrex screw-cap tube containing 0.5 ml of water. This mixture was then partitioned twice with 5 ml hexane, and the combined hexane layers were evaporated to dryness with gaseous nitrogen. Samples were resuspended in 0.2 ml of methanol:dichloromethane (10:1, vol/vol) and reduced with 20 µl of 200 mM $NaBH_4$ prepared in 100% ethanol. Samples were then centrifuged (5 min; 21,000×*g*), and 50 µl aliquots were immediately injected on a Supelco Discovery C-18 column (250 × 4.6 mm; 5 µM) held at 30 °C and developed at a flow rate of 1 ml min^{-1} with methanol:hexane (90:10, vol/vol). Ubiquinol-9 (9.7 min) and ubiquinol-10 (12.3 min) were monitored at 290 nm, while ubiquinone-10 (17.4 min) was monitored at 275 nm. Quinols and quinones were quantified according to their respective external standards, and ubiquinone-9 amounts were corrected for the recovery and the reoxidation of the ubiquinone-10 internal standard. For the quantification of *de novo* ubiquinone-9 biosynthesis in [^{13}C-*ring*]-phenylalanine-fed *A. thaliana*, 50–120 mg of fresh weight leaves were spiked with 86 pmoles of ubiquinone-10 as an internal standard. The samples were then ground, extracted and resuspended in methanol:dichloromethane (10:1, v/v) as described above. The samples (5 µl aliquots) were chromatographed on a Zorbax SB-C18 rapid resolution HT column (50 mm × 2.1 mm; 1.8 µm; Agilent Technologies) held at 40 °C and developed at 0.4 ml min^{-1} with 100% methanol containing 5 mM ammonium formate. The eluate was electrosprayed in positive mode with gaseous nitrogen (300 °C) at a flow rate of 10 L min^{-1} into an Agilent 6430 Triple Quadrupole mass spectrometer. Nebulizer pressure was 35 psi and capillary potential voltage was set to 4000V. Quinols and quinones were analyzed by multiple reaction monitoring using dwell time of 50 ms and the following ion pairs: ubiquinol-9 (814.6/197) and [$^{13}C_6$ *ring*]-ubiquinol-9 (820.6/203) at 3.9 min, ubiquinol-10 (882.7/197) and [$^{13}C_6$ *ring*]-ubiquinol-10 (888.7/203) at 6.5 min, ubiquinone-9 (812.6/197) and [$^{13}C_6$ *ring*]-ubiquinone-9 (818.6/203) at 8.0 min, ubiquinone-10 (880.7/197) and [$^{13}C_6$ *ring*]-ubiquinone-10 (886.7/203) at 13.7 min.

4.4. Extraction, de-glycosylation and analysis of 4-hydroxybenzoate

Leaves and roots (100 mg) were homogenized in 300 µl of methanol:water (90:10, vol/vol) using a 5 ml Pyrex tissue grinder. The grinder was then washed with 300 µl of methanol:water (90:10, vol/vol), and the wash was combined to the original extract. The samples were cleared by centrifugation (10 min; 21,000×*g*), and the supernatants were mixed with 700 µl of 2.6 N HCl. After 1 h incubation at 70 °C, 200 µl aliquots of the hydrolysates were mixed with 100 µl of 100% (vol/vol) methanol and centrifuged (10 min; 21,000×*g*). Samples (300 µl) were then phase-partitioned twice with 2 ml of 100% ethyl acetate. The ethyl acetate phases were then evaporated to dryness, and the samples were resuspended overnight at 4 °C in 300 µl of 10 mM sodium acetate (pH 5.5):methanol (90:10, vol/vol). Samples were centrifuged (10 min; 21,000×*g*) prior to HPLC analysis on a Zorbax Eclipse Plus C18 column (4.6 × 100 mm; 3.5 µm; Agilent Technologies) held at 30 °C. The column was developed in isocratic mode at a flow rate of 0.8 ml min^{-1} with 95% solvent A (10 mM sodium acetate, pH 3.5) and 5% solvent B (100% methanol). 4-hydroxybenzoate (retention time 3.4 min) was detected spectrophotometrically (246 nm) and was quantified according to external calibration standards.

Declaration of competing interest

The authors declare that they have no known competing financial interests or personal relationships that could have appeared to influence the work reported in this paper.

Acknowledgement

This work was made possible in part by National Science Foundation Grant MCB-1712608 (G.J.B.), GRFP DGE-1842473 (A.C.B.), USDA-ARS project 6036-11210-001-00D (A.K.B), and USDA-ARS Floriculture and Nursery Research Initiative (T.A.C.).

Appendix A. Supplementary data

Supplementary data to this article can be found online at https://doi.org/10.1016/j.phytochem.2021.112738.

References

Bentinger, M., Brismar, K., Dallner, G., 2007. The antioxidant role of coenzyme Q. Mitochondrion 7S, S41–S50. https://doi.org/10.1016/j.mito.2007.02.006.

Bentinger, M., Tekle, M., Dallner, G., 2010. Coenzyme Q - biosynthesis and functions. Biochem. Biophys. Res. Commun. 396, 74–79. https://doi.org/10.1016/j.bbrc.2010.02.147.

Block, A., Widhalm, J.R., Fatihi, A., Cahoon, R.E., Wamboldt, Y., Elowsky, C., Mackenzie, S.A., Cahoon, E.B., Chapple, C., Dudareva, N., Basset, G.J., 2014. The origin and biosynthesis of the benzenoid moiety of ubiquinone (Coenzyme Q) in Arabidopsis. Plant Cell 26, 1938–1948. https://doi.org/10.1105/tpc.114.125807.

Brandt, U., Trumpower, B., 1994. The protonmotive Q cycle in mitochondria and bacteria. Crit. Rev. Biochem. Mol. Biol. 29, 165–197. https://doi.org/10.3109/10409239409086800.

Buer, C.S., Kordbacheh, F., Truong, T.T., Hocart, C.H., Djordjevic, M.A., 2013. Alteration of flavonoid accumulation patterns in transparent testa mutants disturbs auxin transport, gravity responses, and imparts long-term effects on root and shoot architecture. Planta 238, 171–189. https://doi.org/10.1007/s00425-013-1883-3.

Cooper-Driver, G., Corner-Zamodits, J.J., Swain, T., 1972. The metabolic fate of hydroxybenzoic acids in plants. Z. Naturforsch. 27 b, 943–946. https://doi.org/10.1515/znb-1972-0817.

Dawson, R.M.C., Elliot, D.C., Elliot, W.H., Jones, K.M., 1986. Data for Biochemical Research. Oxford University Press, New York.

Fernández-Del-Río, L., Nag, A., Gutierrez Casado, E., Ariza, J., Awad, A.M., Joseph, A.I., Kwon, O., Verdin, E., de Cabo, R., Schneider, C., Torres, J.Z., Burón, M.I., Clarke, C. F., Villalba, J.M., 2017. Kaempferol increases levels of coenzyme Q in kidney cells and serves as a biosynthetic ring precursor. Free Radic. Biol. Med. 110, 176–187. https://doi.org/10.1016/j.freeradbiomed.2017.06.006.

Fernández-Del-Río, L., Soubeyrand, E., Basset, G.J., Clarke, C.F., 2020. Metabolism of the flavonol kaempferol in kidney cells liberates the B-ring to enter Coenzyme Q biosynthesis. Molecules 25, 2955. https://doi.org/10.3390/molecules25132955.

Jones, P., Messner, B., Nakajima, J., Schäffner, A.R., Saito, K., 2003. UGT73C6 and UGT78D1, glycosyltransferases involved in flavonol glycoside biosynthesis in *Arabidopsis thaliana*. J. Biol. Chem. 278, 43910–43918. https://doi.org/10.1074/jbc.M303523200.

Klick, S., Herrmann, K., 1988. Glucosides and glucose esters of hydroxybenzoic acids in plants. Phytochemistry 27, 2177–2180. https://doi.org/10.1016/0031-9422(88)80121-3.

Lepiniec, L., Debeaujon, I., Routaboul, J.M., Baudry, A., Pourcel, L., Nesi, N., Caboche, M., 2006. Genetics and biochemistry of seed flavonoids. Annu. Rev. Plant Biol. 57, 405–430. https://doi.org/10.1146/annurev.arplant.57.032905.105252.

Lim, E.K., Doucet, C.J., Li, Y., Elias, L., Worrall, D., Spencer, S.P., Ross, J., Bowles, D.J., 2002. The activity of Arabidopsis glycosyltransferases toward salicylic acid, 4-hydroxybenzoic acid, and other benzoates. J. Biol. Chem. 277, 586–592. https://doi.org/10.1074/jbc.M109287200.

Liu, M., Chen, X., Wang, M., Lu, S., 2019. SmPPT, a 4-hydroxybenzoate polyprenyl diphosphate transferase gene involved in ubiquinone biosynthesis, confers salt tolerance in *Salvia miltiorrhiza*. Plant Cell Rep. 38, 1527–1540. https://doi.org/10.1007/s00299- 019-02463-5.

Nowicka, B., Kruk, J., 2010. Occurrence, biosynthesis and function of isoprenoid quinones. Biochim. Biophys. Acta 1797, 1587–1605. https://doi.org/10.1016/j.bbabio.2010.06.007.

Ohara, K., Kokado, Y., Yamamoto, H., Sato, F., Yazaki, K., 2004. Engineering of ubiquinone biosynthesis using the yeast *coq2* gene confers oxidative stress tolerance in transgenic tobacco. Plant J. 40, 734–743. https://doi.org/10.1111/j.1365-313X.2004.02246.x.

Pierrel, F., Hamelin, O., Douki, T., Kieffer-Jaquinod, S., Mühlenhoff, U., Ozeir, M., Lill, R., Fontecave, M., 2010. Involvement of mitochondrial ferredoxin and para-aminobenzoic acid in yeast coenzyme. Q biosynthesis. Chem. Biol. 17, 449–459. https://doi.org/10.1016/j.chembiol.2010.03.014.

Schoenbohm, C., Martens, S., Eder, C., Forkmann, G., Weisshaar, B., 2000. Identification of the *Arabidopsis thaliana* flavonoid 3'-hydroxylase gene and functional expression of the encoded P450 enzyme. Biol. Chem. 381, 749–753. https://doi.org/10.1515/BC.2000.095.

Siebert, M., Sommer, S., Li, S.M., Wang, Z.X., Severin, K., Heide, L., 1996. Genetic engineering of plant secondary metabolism. Accumulation of 4-hydroxybenzoate glucosides as a result of the expression of the bacterial ubiC gene in tobacco. Plant Physiol. 112, 811–819. https://doi.org/10.1104/pp.112.2.811.

Soubeyrand, E., Johnson, T.S., Latimer, S., Block, A., Kim, J., Colquhoun, T.A., Butelli, E., Martin, C., Wilson, M.A., Basset, G.J., 2018. The peroxidative cleavage of kaempferol contributes to the biosynthesis of the benzenoid moiety of ubiquinone in plants. Plant Cell 30, 2910–2921. https://doi.org/10.1105/tpc.18.00688.

Soubeyrand, E., Kelly, M., Keene, S.A., Bernert, A.C., Latimer, S., Johnson, T.S., Elowsky, C., Colquhoun, T.A., Block, A.K., Basset, G.J., 2019. Arabidopsis 4-COUMAROYL-COA LIGASE 8 contributes to the biosynthesis of the benzenoid ring of coenzyme Q in peroxisomes. Biochem. J. 476, 3521–3532. https://doi.org/10.1042/BCJ20190688.

Tohge, T., Nishiyama, Y., Hirai, M.Y., Yano, M., Nakajima, J., Awazuhara, M., Inoue, E., Takahashi, H., Goodenowe, D.B., Kitayama, M., Noji, M., Yamazaki, M., Saito, K., 2005. Functional genomics by integrated analysis of metabolome and transcriptome of Arabidopsis plants over-expressing an MYB transcription factor. Plant J. 42, 218–235. https://doi.org/10.1111/j.1365-313X.2005.02371.x.

Yazaki, K., Inushima, K., Kataoka, M., Tabata, M., 1995. Intracellular localization of UDPG: *p* - hydroxybenzoate glucosyltransferase and its reaction product in Lithospermum cell cultures. Phytochemistry 38, 1127–1130. https://doi.org/10.1016/0031-9422(94)00821-A.

Yin, R., Messner, B., Faus-Kessler, T., Hoffmann, T., Schwab, W., Hajirezaei, M.R., von Saint Paul, V., Heller, W., Schäffner, A.R., 2012. Feedback inhibition of the general phenylpropanoid and flavonol biosynthetic pathways upon a compromised flavonol-3-O- glycosylation. J. Exp. Bot. 63, 2465–2478. https://doi.org/10.1093/jxb/err416.

Yin, R., Han, K., Heller, W., Albert, A., Dobrev, P.I., Zažímalová, E., Schäffner, A.R., 2014. Kaempferol 3-*O*-rhamnoside-7-*O*-rhamnoside is an endogenous flavonol inhibitor of polar auxin transport in Arabidopsis shoots. New Phytol. 201, 466–475. https://doi.org/10.1111/nph.12558.

Yonekura-Sakakibara, K., Tohge, T., Niida, R., Saito, K., 2007. Identification of a flavonol 7-*O*- rhamnosyltransferase gene determining flavonoid pattern in Arabidopsis by transcriptome coexpression analysis and reverse genetics. J. Biol. Chem. 282, 14932–14941. https://doi.org/10.1074/jbc.M611498200.

Yonekura-Sakakibara, K., Tohge, T., Matsuda, F., Nakabayashi, R., Takayama, H., Niida, R., Watanabe-Takahashi, A., Inoue, E., Saito, K., 2008. Comprehensive flavonol profiling and transcriptome coexpression analysis leading to decoding gene-metabolite correlations in Arabidopsis. Plant Cell 20, 2160–2176. https://doi.org/10.1105/tpc.108.058040.